Experimental Investigation of Inverter Open-Circuit Fault Diagnosis for Bi-Harmonic Five-Phase Permanent Magnet Drive

[(1)]Mohamed Trabelsi, Member, IEEE, [(1)]Eric Semail, Member IEEE, and [(1)]Ngac Ky Nguyen, Member, IEEE

[(1)]Univ. Lille, Centrale Lille, Arts et Metiers ParisTech, HEI, HeSam, EA 2697 - L2EP - Laboratoire d'Electrotechnique et d'Electronique de Puissance, F-59000 Lille, France.
E-mails: mohamed.trabelsi@ensam.eu, eric.semail@ensam.eu, ngacky.nguyen@ensam.eu

This work has been achieved within the framework of CE2I project (Convertisseur d'Energie Intégré Intelligent). CE2I is co-financed by European Union with the financial support of European Regional Development Fund (ERDF), French State and the French Region of Hauts-de-France.

The authors are with the Universite Lille, Centrale Lille, Arts et Metiers ParisTech, HEI, HeSam, EA 2697-L2EP-Laboratoire d'Electrotechnique et d'Electronique de Puissance F-59000, Lille, France (e-mail: mohamed. trabelsi@ensam.eu; eric.semail@ensam.eu; ngacky.nguyen@ensam.eu).

Abstract—This paper proposes a procedure that is suitable for experimental investigation of real-time open-switch and open-phase faults diagnosis of a five-leg Voltage Source Inverter (VSI) feeding a five-phase bi-harmonic Permanent Magnet Synchronous Machine (5-Φ B-PMSM). The algorithm is based on the specific characteristics of multiphase machines, which allows inverter fault detection with sufficient robustness of the algorithm in the presence of fundamental and third harmonic components. Firstly, the inverter fault effects analysis is achieved in the characteristic subspaces of the five-phase PMSM. Specificities that are interesting for the elaboration of a real-time Fault Detection and Identification (FDI) process are highlighted. Original and particular algorithms are used for an accurate two-dimensional normalized fault vector extraction in a defined fault reference frame. This frame is dedicated only for fault detection and identification. To ensure the high immunity of the FDI process against transient states, a particular normalization procedure is applied. The normalized diagnostic signals are formulated from the defined frame and others variables derived from the reference and measured currents. Simulation and experimental results of open-switch and open-phase faults are provided to validate the proposed algorithm.

Index Terms—Space vector theory, multiphase systems, fault diagnosis, five-phase permanent magnet synchronous machine, inverter open-circuit fault.

NOMENCLATURE

i_n	Phase currents in natural frame *abcde*
$i_{\alpha\beta}$, i_{xy}	Current components in α-β and x-y frames
Ω	Mechanical rotor speed
F_d	Diagnostic variable used for fault detection
F_i	Diagnostic variable used for fault identification
r_{nN}	Diagnostic variable used for open-phase fault identification
VSI	Voltage Source Inverter
OSF	Open Switch Fault
OPF	Open Phase Fault
OSG	Open Switch Group
OPG	Open Phase Group
PWM	Pulse Width Modulation
FDI	Fault Detection and Identification
Back-EMF	Back Electromotive Force
FFT	Fast Fourier Transform
2D	Two Dimensional
5-Φ B-PMSM	Five-phase Bi-harmonic PMSM

I. INTRODUCTION

Because of their fault-tolerance and high power density, variable-speed drives based on 5-Φ PMSMs are gaining importance in several very sensitive applications such as automotive [1], aerospace [2], ship and offshore turbine [3]. In these applications, the drive system is exposed to hard operating conditions. In addition to the natural aging process, these conditions may lead to several faults that are essentially related to the machines or the Voltage Source Inverters (VSIs). The VSI system alone is considered as one of the most sensitive parts in the electromechanical conversion chain. Moreover, the power switches and the electronic control boards are also considered as the main sources of their failures [4]-[5]. Hence, aging and degradation result in short-circuit fault or open-circuit fault of the power switches. In this paper only open-circuit fault is studied, considering that short-circuit, which usually cannot be tolerated, leads to open-circuit fault. Even if by principle a fault-tolerant multiphase drive can continue to work under fault conditions, impacts can be significant in terms of oversizing, induced torque ripples and vibrations. Consequently, a post-fault operation without reconfiguration can lead to severe secondary faults in the other parts of the system [6]. Therefore, fault detection is useful in order to adopt a control reconfiguration [7]-[8].

Most addressed approaches for open-switch faults diagnosis concern classical three-phase machines. Their evaluation and classification have been addressed in [6] and [9]. The method proposed in this paper belongs to the family of the signal-based methods [9] and especially considering only current signals, as in [12]-[17] and [21]-[22]. Methods based on voltage signals are not considered in this work since they require additional voltage sensors, as addressed in [10]-[11], or observers development, as proposed in [18]-[20].

In [14] and [15], the diagnostic algorithms have been proposed for OSF in the case of sinusoidal 3-Φ PMSM. In order to detect the faulty switches, the average values of the current errors and/or the average absolute current values were used to formulate the diagnostic variables. However, it has been shown that the OSF occurrence in one inverter leg results in symmetrical fault current quantities across the two other healthy phases. This characteristic together with the accurate chosen diagnostic variables allowed a robust fault detection in these classical 3-Φ systems. Unfortunately, these methods become inapplicable to the 5-Φ PMSM due to the asymmetrical distribution of the fault current quantities in the healthy phases after the fault occurrence (these assertions are addressed in section II-B). The method proposed in [16] used the current error value with additional variables to detect the OSF occurrence in the VSI. This method was applied to a 3-Φ BLDC motor. However, it was based on the operating characteristics of these motor types with trapezoidal back-EMFs and square phase currents. Consequently, this method is inapplicable to the 5-Φ B-PMSM under study.

In [17]-[20], the diagnostic methods have been accomplished based on model reference systems paralleled with the drive to generate residual signals having information on the fault occurrence in the VSI feeding 3-Φ motors. Several estimator and observer types were used. To detect the fault, a directional residual evaluation was performed in natural frame *abc* as well as in *α-β* frame. Although they do not require extra hardware, the robustness and effectiveness of these methods depend on the accuracy of the estimation of the model parameters. In addition, if these approaches are used for 5-Φ B-PMSM systems, they imply at least two *dq*-machine models with more electrical parameters in comparison to 3-Φ systems. A large number of parameters may affect the robustness and increase the complexity and the computational effort.

The research works dedicated to the power switch fault diagnosis in multiphase drives are still very limited [21]-[22]. In [21], the diagnostic algorithm is defined for a BLDC five-machine supplied by the first and third harmonics of currents. The proposed approach is based on an adaptive RLS (Recursive Less Square) identification of each measured current. Errors between the output of adaptive estimation and the one obtained by the model are used for detection. However, in addition to the parameters dependency, using an adaptive estimator for each phase greatly increases the computation time. In [23] and [24], for almost sinusoidal five-phase machines, it is shown clearly, as in [22], that the inverter fault induces a fault current component in the second plane instead of a near zero current component under a healthy operation of the VSI. Accordingly, the technique addressed in [22] is successfully applied to these almost sinusoidal 5-Φ PMSM ($\rho \leq 20$ %). However, when considering the 5-Φ B-PMSM, the

robustness of this technique is low because of the existence of the significant third harmonic current component used essentially to produce the torque, as illustrated in [25]-[26].

This paper is based on Concordia-frame for the fault detection and Park-frame for the control. It addresses the problem of fault detection and identification in the case of bi-harmonic multiphase machines supplied normally with two significant current harmonics, and it is effective also for the sinusoidal multiphase machines. The proposed technique uses data available in the two α-β and x-y planes. Using an innovative and particular algorithm, a two dimensional fault vector is defined with fault variables and, when a fault appears, it describes, in an α_f-β_f fault reference plane defined only for fault diagnosis, a non-zero trajectory characterizing the fault in the VSI. Moreover, an original normalization procedure is also proposed to facilitate the fault diagnosis and to ensure the high immunity of the FDI process against transient states.

The paper is organized as follows. First the current model under a healthy condition and the effects of open-switch and open-phase faults on the 5-Φ B-PMSM are presented in section II. Section III defines the primitive fault vector in natural frame. Section IV derives an accurate fault vector extraction method in α_f-β_f fault reference frame. The principle of the fault diagnosis is presented in section V. Section VI provides the experimental results to confirm the effectiveness and robustness of the proposed FDI process.

II. Features of Pre- and Post-Fault Operation of the 5-Φ B-PMSM

A schematic diagram of the considered overall electrical drive system including the 5-leg VSI is depicted in Fig.1. The analysis is performed regarding the phase currents under healthy and faulty conditions of the VSI. The effects of inverter open-circuit faults are analyzed in natural frame *abcde* and in the orthogonal frames α-β and x-y. All results are obtained in closed-loop vector control with PI controllers working in dq-rotating frames.

A. Pre-Fault Current Model

In natural frame *abcde*, the phase currents of 5-Φ B-PMSM, $i_n(t)$, can be expressed as

$$i_n(t) = I_{h1}\sin\left(p\Omega t-(n-1)\frac{2\pi}{5}\right)-I_{h3}\sin\left(3\left(p\Omega t-(n-1)\frac{2\pi}{5}\right)\right) \quad (1)$$

n = 1,...,5 denotes the phase currents (i_a, i_b, i_c, i_d, and i_e), I_{h1} and I_{h3} are the magnitudes of the first and third current harmonics, respectively. $p\Omega$ is the electrical instantaneous fundamental frequency. The current components, in α-β and x-y frames, are obtained by

$$\left[i_{\alpha\beta}\right]=\left[C_{\alpha\beta}\right]\left[i_n\right]^t \quad (2)$$

$$\left[i_{xy}\right]=\left[C_{xy}\right]\left[i_n\right]^t \quad (3)$$

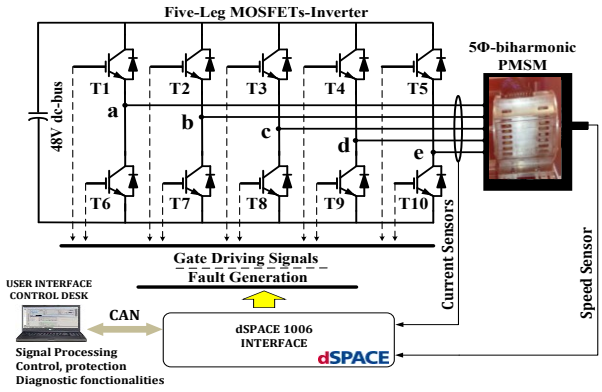

Fig.1. Configuration of the considered electrical drive system.

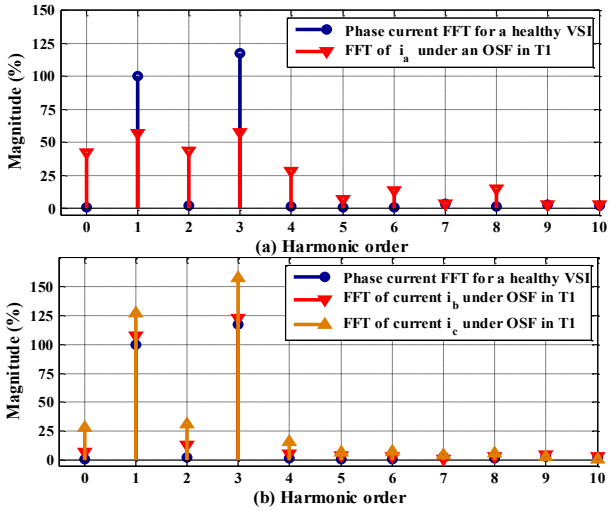

Fig. 2. Experimental results. Comparison of the harmonic content of three out of five phase currents for a healthy inverter and when an open switch fault occurs in the 5-leg VSI. (a) Comparison of the faulty phase *a* current with a healthy current. (b) Comparison of the phase *b* and *c* currents with a healthy current.

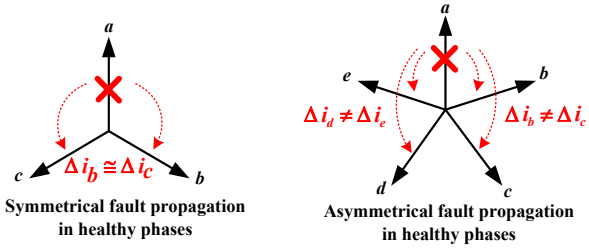

Fig.3. Comparison of fault propagation way in classical three-phase machines and five-phase machines.

$\left[C_{\alpha\beta}\right]$ and $\left[C_{xy}\right]$, defined in (4)-(5), denote the five phase Concordia transformation. Here, it should be noticed that there is no path for the zero-sequence current because of the isolated star connection of the PMSM.

$$\left[C_{\alpha\beta}\right]=\sqrt{\frac{2}{5}}\begin{bmatrix}1 & \cos\frac{2\pi}{5} & \cos\frac{4\pi}{5} & \cos\frac{6\pi}{5} & \cos\frac{8\pi}{5}\\ 0 & \sin\frac{2\pi}{5} & \sin\frac{4\pi}{5} & \sin\frac{6\pi}{5} & \sin\frac{8\pi}{5}\end{bmatrix} \quad (4), \qquad \left[C_{xy}\right]=\sqrt{\frac{2}{5}}\begin{bmatrix}1 & \cos\frac{4\pi}{5} & \cos\frac{8\pi}{5} & \cos\frac{12\pi}{5} & \cos\frac{16\pi}{5}\\ 0 & \sin\frac{4\pi}{5} & \sin\frac{8\pi}{5} & \sin\frac{12\pi}{5} & \sin\frac{16\pi}{5}\end{bmatrix} \quad (5)$$

Substituting (4) and (5) into (2) and (3) results in the α-β and x-y axis currents as

$$i_{\alpha\beta}(t)=\begin{cases}\sqrt{\frac{5}{2}}I_{h1}\sin\left(p\Omega t\right)\\ \sqrt{\frac{5}{2}}I_{h1}\sin\left(p\Omega t-\frac{\pi}{2}\right)\end{cases} \quad (6), \qquad i_{xy}(t)=\begin{cases}\sqrt{\frac{5}{2}}I_{h3}\sin\left(-3p\Omega t\right)\\ \sqrt{\frac{5}{2}}I_{h3}\sin\left(-3\left(p\Omega t-\frac{\pi}{2}\right)\right)\end{cases} \quad (7)$$

Under a healthy operation of the VSI, the shapes built by the currents in α-β and x-y frames are two circles centered at the origin with a radius equal to the magnitude of the first harmonic component and third harmonic component, respectively.

B. Post-Fault Current Analysis

In Fig.2, the spectrograms of the phase currents in three out of five windings of the 5-Φ B-PMSM (only phases *a*, *b* and *c*) are presented under healthy conditions and under an open-switch fault of transistor T1. The currents in the phases *d* and *e* can be deduced by symmetry considerations from the currents in the phases *b* and *c*. For a healthy

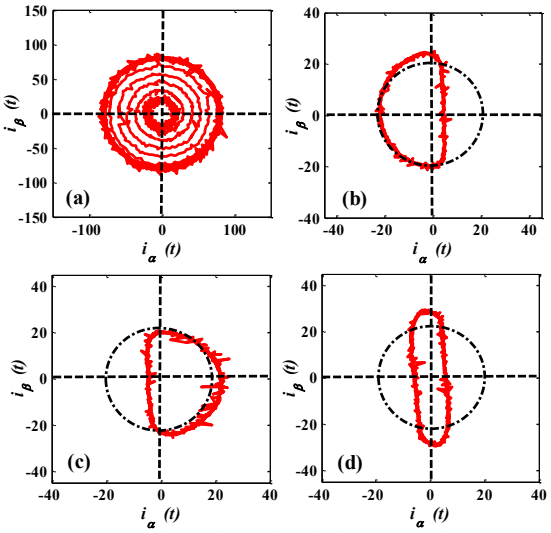

Fig. 4. Experimental results of the OSF and OPF effects analysis on a 5-Φ B-PMSM in orthogonal *α-β* frame. (a) Healthy operation mode and a step increase of the load torque. (b) OSF in T1. (c) OSF in T6. (d) OPF (T1 and T6 are involved).

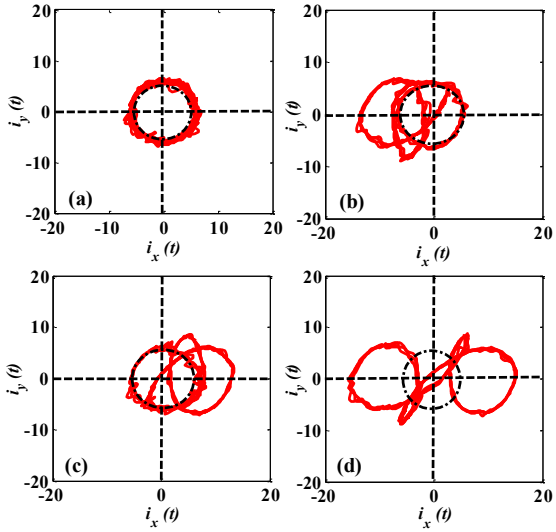

Fig. 5. Experimental results of the OSF and OPF effects analysis on a 5-Φ B-PMSM in orthogonal *x-y* frame. (a) Healthy operation mode. (b) OSF in T1. (c) OSF in T6. (d) OPF (T1 and T6 are involved).

operation mode, the harmonic content of phase current is well known and contains only the first and third harmonic components, as defined in equation (1). On the contrary, the fault occurrence in transistor T1, results in several supplementary even harmonic components induced in all phase currents. Regarding the two healthy phase currents (phase *b* and phase *c* in Fig.2-b), it can be observed that their harmonic contents are modified differently since the variations of the magnitudes are not the same: an asymmetry appears between the remaining healthy phases. This means that the fault induces at least two different signals for a five-phase machine instead of one for a wye-coupled three-phase machine. In Fig.3, it is clearly shown that, in the case of the 5-Φ PMSM, the current fault quantities across the healthy phases ($\Delta i_b \neq \Delta i_c$) are not the same in comparison with the classical three-phase system in which the fault quantity is symmetrically divided between the two healthy phases ($\Delta i_b \cong \Delta i_c$). It is the reason why a direct analysis in natural frame *abcde*, for diagnostic purposes, will be difficult. Hence, the particular behavior of the system under study must be considered for designing the FDI process.

Now, when working with the 5-Φ B-PMSM, there are two orthogonal frames which are available for the analysis instead of one for a 3-Φ PMSM. Experimental results of the OSF and OPF effects analysis in *α-β* and *x-y* frames are

shown in Fig. 4 and Fig. 5. In comparison to the healthy operation mode, after the fault occurrence, the shapes are no more circles and each fault induces different trajectories in both planes α-β and x-y. Unfortunately, in these frames, the obtained shapes are dominated by the fundamental harmonics that are used to produce the torque, resulting in more complexity and low robustness of the real-time FDI process. Nevertheless, a significant feature, for the system under study, is the fact that the first harmonic is decoupled from the third one. Consequently, there is no path of the third harmonic component in α-β frame. This allows the improvement of the diagnostic technique immunity against false alarms. On the other hand, the projected components, in α-β frame, cannot be used directly without preconditioning for real-time fault diagnosis of open-switch faults because of the mechanical load dependency due to the presence of the first harmonic component.

Experimental results depicted in Fig. 6 provide the dynamic behavior of the reference and measured phase currents during fault occurrence in the VSI. The considered fault scenario is an open-switch fault in the upper transistor T_{n}. Considering the closed-loop vector control of the 5-Φ B-PMSM, speed and current controllers cannot be able to achieve zero errors under fault conditions. This is due to the inability of the speed and current controllers to compensate the physical fault in the VSI resulting from the unbalanced faulty system. Consequently, the reference currents and the measured ones cannot have the same dynamic behavior after the fault occurrence, as reported in Fig. 6. It is the reason why, as opposed to the classical diagnostic methods, the normalization step in the FDI process must be achieved independently to take into account the real-time dynamic of the system and improve the immunity against false alarms.

The next sections discuss the main steps to design a high performance real-time FDI process with respect to the method's effectiveness, the robustness against transient states and the independency of the fundamental current harmonic components and the electric drive parameters variation.

III. Primitive Fault Vector Definition in Natural Frame

As illustrated in Fig. 6, for a healthy condition, reference and measured currents have the same dynamic behavior and are flowing in positive and negative directions. On the contrary, under an open-switch fault of T_n, the fault occurrence limits the measured phase current i_{n_m} to flow only in the negative direction during a half current period, since the positive wave of the current cannot be shaped. Here, it should be noticed that if the fault occurs in the lower transistor T_{n+5}, the negative wave of the measured current cannot be shaped. In this case, i_{n_m} will present only a positive direction during half a current period. Regarding the reference phase current, it is observed that it is always

flowing in positive and negative directions. Consequently, the primitive fault components in natural frame *abcde* can be defined as the residual quantities between the reference currents and the measured ones as follows:

$$f_n(t) = i_{nref}(t) - i_{n\_m}(t) \qquad (8)$$

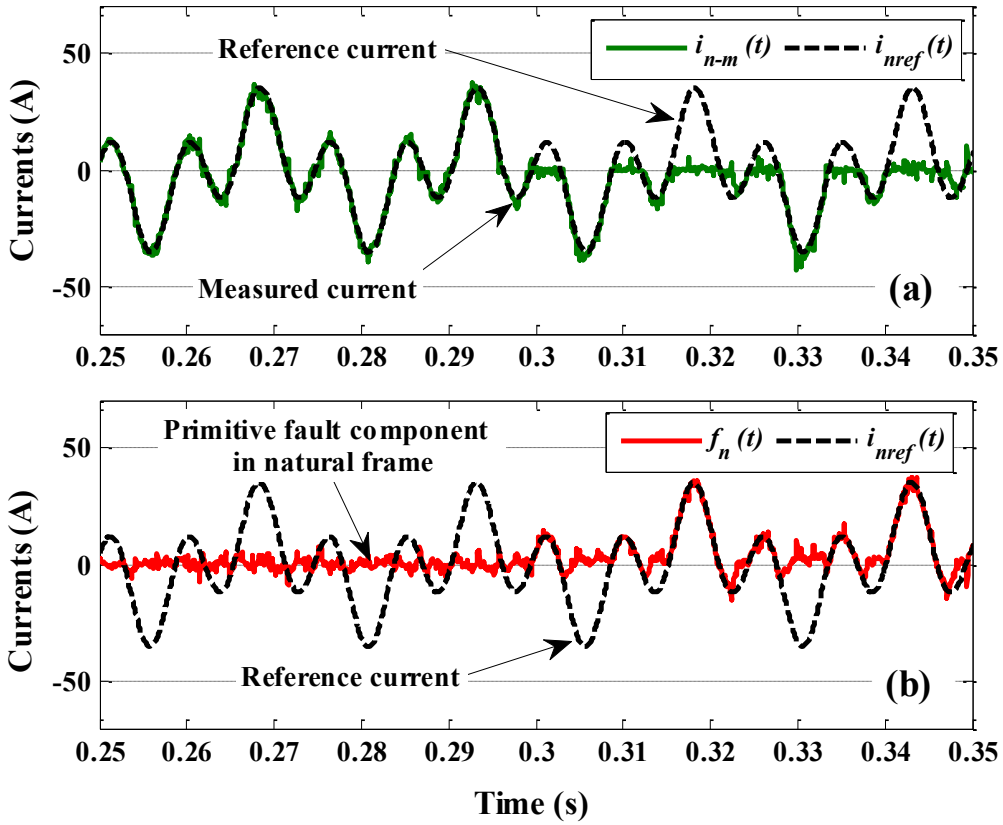

Fig. 6. Experimental results of the 5-Φ B-PMSM under an open-circuit fault in transistor T_n (n = 1, 2, 3, 4, 5). (a) Reference and measured currents in natural frame *abcde*. (b) Reference current and primitive fault component in natural frame *abcde*. f = 40 Hz , (for the first harmonic frequency) and I_{h3}=1.22×I_{h1}

where, i_{n_m} denotes the measured phase current. i_{nref} are the reference phase currents (of the healthy mode) and $f_n = (f_1, f_2, f_3, f_4, f_5)$, respectively associated with the phases (*a, b, c, d, e*), are the fault current quantities corresponding to each phase of the 5-Φ B-PMSM. In healthy mode, with vector control in rotating frames, it is easy to ensure, in steady state and even during speed transients in accordance with current bandwidth control, that the errors are equal to zero when the VSI can impose the four currents. Based on result in Fig. 6, the variable $f_n(t)$ can be approximated, according to the OSF location, as a function of the first and third harmonic components by

- If T_n is faulty

$$f_n(t)=\begin{cases} I_{h1}\sin\left(p\Omega t-(n-1)\frac{2\pi}{5}\right)+I_{h3}\sin\left(-3\left(p\Omega t-(n-1)\frac{2\pi}{5}\right)\right) \\ \qquad for \quad (n-1)\frac{2\pi}{5}\le \omega t \le \pi+(n-1)\frac{2\pi}{5}, \\ 0, \qquad for \quad \pi+(n-1)\frac{2\pi}{5}\le \omega t \le 2\pi+(n-1)\frac{2\pi}{5} \end{cases} \quad (9),$$

- If T_{n+5} is faulty

$$f_n(t)=\begin{cases} 0, \qquad for \quad (n-1)\frac{2\pi}{5}\le \omega t \le (n-1)\frac{2\pi}{5}+\pi \\ I_{h1}\sin\left(p\Omega t-(n-1)\frac{2\pi}{5}\right)+I_{h3}\sin\left(-3\left(p\Omega t-(n-1)\frac{2\pi}{5}\right)\right) \\ \qquad for \quad \pi+(n-1)\frac{2\pi}{5}\le \omega t \le 2\pi+(n-1)\frac{2\pi}{5}, \end{cases} \quad (10)$$

Substituting these expressions into (8) and using the linear transformation (4) and (5), it is easy to define the equivalent fault quantities in α-β and x-y frames. In these frames, the obtained analytical expressions derived from (8) will help to study the open-switch fault in 5-Φ B-PMSM system with sufficient accuracy and to define a high performance real-time FDI process.

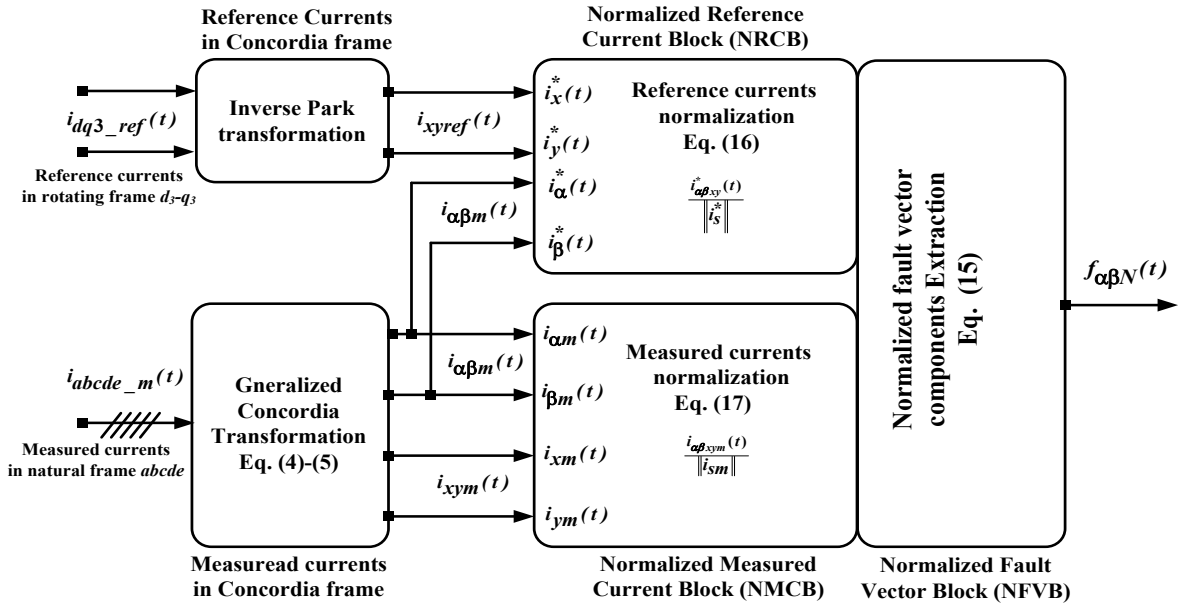

Fig.7. Proposed technique for fault components extraction in α_f-β_f fault reference frame for a closed-loop control of the 5-Φ B-PMSM.

IV. Accurate Fault Vector Extraction in α_f-β_f Fault Reference Frame

The first choice in this work is to consider that the FDI process will be achieved by considering only a two-dimensional (2D) fault vector whose trajectory analysis in a plane called "α_f-β_f fault reference frame" will give a convenient information for the fault diagnosis. However, from four-dimensional (4D) reference and measured current vectors, new 2D variables, sensitive to fault are elaborated with a main constraint. This constraint is that the 2D vector must be equal to zero in normal operation. Errors between 4D reference and measured current vectors will be thus included in the 2D fault vector.

The second choice in the elaboration of the FDI process is to consider a normalized fault vector. The reason is that the fault diagnosis algorithm must operate not only in steady state operation but also in transient states without causing false alarms.

The proposed algorithm to achieve these goals is depicted in Fig. 7. It is used to define the α_f-β_f fault reference frame. In this frame, the 2D normalized fault vector ($f_{\alpha N}$, $f_{\beta N}$) is calculated. Since the proposed particular strategy makes it possible to avoid the two fundamental current harmonics propagation in α_f-β_f fault reference frame used for fault diagnosis, it guarantees the independency of the 5-Φ B-PMSM parameters variation and the mechanical load transient states. In order to generate only the fault vector components in α_f-β_f fault reference frame, it is necessary to

- use the available reference currents, derived from the outer control loop that provides the reference currents to the current controllers, together with the measured phase currents;
- connect permanently the input reference currents $i^*_{\alpha\beta}$ to $i_{\alpha\beta m}$. This particular connection involves the same current (1st harmonic) at the input of the NRCB block and the NMCB block;
- normalize independently the reference currents and the measured ones since they have a different dynamic behavior under fault condition, as illustrated in Fig. 6.

The reference and the measured currents, in α-β and x-y frames, are obtained considering the inverse Park and linear Concordia transformations, respectively. Considering Fig. 7, the general form of all inputs of the proposed algorithm are expressed as

- for the inputs of the NRCB block

$$\begin{aligned} i^*_{\alpha\beta}(t) &= i_{\alpha\beta m}(t) \\ i^*_{xy}(t) &= i_{xyref}(t) = \left[P(3\theta)\right]^{-1}\left[i_{dq3\_ref}\right]^t \end{aligned} \tag{11}$$

- for the inputs of the NMCB block

$$\begin{aligned} i_{\alpha\beta m}(t) &= \left[C_{\alpha\beta}\right]\left[i_{n\_m}(t)\right]^t \\ i_{xym}(t) &= \left[C_{xy}\right]\left[i_{n\_m}(t)\right]^t \end{aligned} \tag{12}$$

where, i_{xyref} are the current components in x-y frame corresponding to the healthy state as defined in (7). i_{dq3_ref} represents the reference current components in rotating frame d_3-q_3. $[P(3\theta)]^{-1}$ is the inverse Park transformation. $i_{\alpha\beta m}$ and i_{xym} denote the measured current components in α-β and x-y frames.

According to the definition of the current fault components in (8), the quantities defined in (12) can be also expressed as

$$i_{\alpha\beta m}(t) = i_{\alpha\beta ref}(t) - f_{\alpha\beta}(t)$$
$$i_{xym}(t) = i_{xyref}(t) - f_{xy}(t) \qquad (13)$$

where, $i_{\alpha\beta ref}$ represents the current components in α-β frame corresponding to the healthy state as defined in (6). $f_{\alpha\beta}(t)$, $f_{xy}(t)$, are the equivalent fault components in α-β and x-y frames expressed in (14) by using (4) and (5) transformations. They are expressed by

$$f_\alpha(t) = \sqrt{\frac{2}{5}} \sum_{n=1}^{5} f_n(t) \cos\left(2(n-1)\frac{\pi}{5}\right); f_\beta(t) = \sqrt{\frac{2}{5}} \sum_{n=1}^{5} f_n(t) \sin\left(2(n-1)\frac{\pi}{5}\right);$$
$$f_x(t) = \sqrt{\frac{2}{5}} \sum_{n=1}^{5} f_n(t) \cos\left(2(n-1)\frac{2\pi}{5}\right); f_y(t) = \sqrt{\frac{2}{5}} \sum_{n=1}^{5} f_n(t) \sin\left(2(n-1)\frac{2\pi}{5}\right) \qquad (14)$$

for n = 1, 2, 3, 4 and 5.

From the two fault vectors $f_{\alpha\beta}(t)$, $f_{xy}(t)$, it is defined an unique normalized fault vector $f_{\alpha\beta N}(t)$. This vector is the output of the NFVB block of fig. 7 and defines a new α_f-β_f fault reference frame. The two components of this normalized fault vector are defined by

$$f_{\alpha N}(t) = \left(\frac{1}{\left\|i_S^*\right\|} - \frac{1}{\|i_{sm}\|}\right) i_{\alpha m}$$
$$f_{\beta N}(t) = \left(\frac{1}{\left\|i_S^*\right\|} - \frac{1}{\|i_{sm}\|}\right) i_{\beta m} \qquad (15)$$

$\left\|i_S^*\right\|$ and $\|i_{sm}\|$ denotes the Concordia modulus of the reference and the measured currents, respectively. They are defined as

$$\left\|i_S^*\right\| = \left(i_{\alpha m}^2 + i_{\beta m}^2 + i_{xref}^2 + i_{yref}^2\right)^{1/2} \qquad (16)$$
$$\|i_{sm}\| = \left(i_{\alpha m}^2 + i_{\beta m}^2 + i_{xm}^2 + i_{ym}^2\right)^{1/2} \qquad (17)$$

In order to highlight the impact of the fault occurrence on the fault vector components $f_{\alpha\beta N}(t)$, a new expression of (15) using only the equivalent fault quantities $f_{\alpha\beta}(t)$, $f_{xy}(t)$ and the reference current components i_{xyref} i_{xyref} is developed below.

Using (13), equations (16) and (17) can be rewritten as

$$\left\|i_S^*\right\| = \left(\left(i_{\alpha ref} - f_\alpha\right)^2 + \left(i_{\beta ref} - f_\beta\right)^2 + i_{xref}^2 + i_{yref}^2\right)^{1/2} \qquad (18)$$
$$\|i_{sm}\| = \left(\left(i_{\alpha ref} - f_\alpha\right)^2 + \left(i_{\beta ref} - f_\beta\right)^2 + \left(i_{xref} - f_x\right)^2 + \left(i_{yref} - f_y\right)^2\right)^{1/2} \qquad (19)$$

Substituting (18) and (19) into equation (15) gives

$$f_{\alpha N}(t)=\frac{1}{A}\left(\frac{1}{\left(1+\frac{i_{xref}^2+i_{yref}^2}{A^2}\right)^{1/2}}-\frac{1}{\left(1+\frac{\left(i_{xref}-f_x\right)^2+\left(i_{yref}-f_y\right)^2}{A^2}\right)^{1/2}}\right)\left(i_{\alpha ref}-f_\alpha\right)$$

$$f_{\beta N}(t)=\frac{1}{A}\left(\frac{1}{\left(1+\frac{i_{xref}^2+i_{yref}^2}{A^2}\right)^{1/2}}-\frac{1}{\left(1+\frac{\left(i_{xref}-f_x\right)^2+\left(i_{yref}-f_y\right)^2}{A^2}\right)^{1/2}}\right)\left(i_{\beta ref}-f_\beta\right) \quad (20)$$

with $A=\left(\left(i_{\alpha ref}-f_\alpha\right)^2+\left(i_{\beta ref}-f_\beta\right)^2\right)^{1/2}$

Based on these expressions, it is demonstrated and concluded that $f_{\alpha N}(t)$, $f_{\beta N}(t)$ and A are functions of the harmonic component amplitudes I_{h1} and I_{h3}. On the other hand, when the optimal Maximum Torque Per Ampere

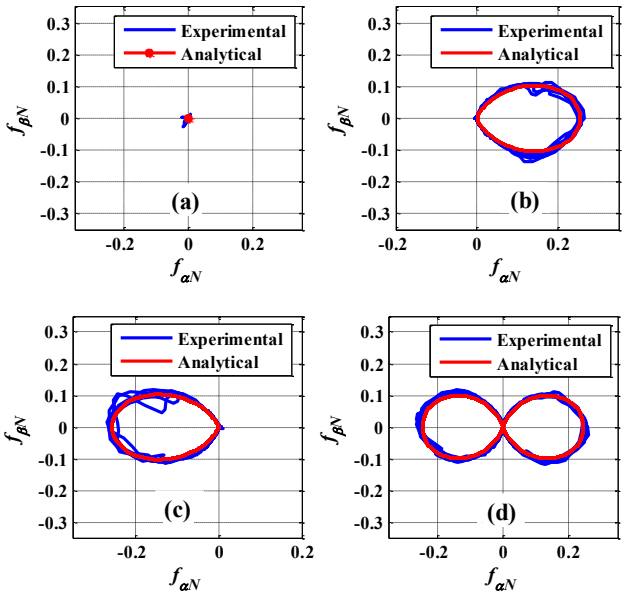

Fig. 8. Fault vector propagation in the defined α_f-β_f fault reference frame. (a) Healthy inverter. (b) Open-switch fault in T1. (c) Open-switch fault in T6. (d) Open-phase fault (T1 and T6).

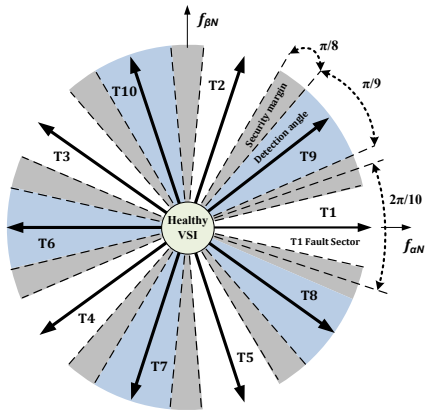

Fig.9. Fault vector average position in α_f-β_f fault reference frame according to the fault location.

(MTPA) strategy is applied to the 5-Φ B-PMSM, the current references i_{d1ref} and i_{d3ref} are equal to zero and the ratio of the third current harmonic component and the first one is the same as the ratio of the third back-EMF harmonic and the first one [28]. As a consequence, I_{h3} can be expressed simply as a fraction of I_{h1} as follows:

$$I_{h3}=\rho.I_{h1} \quad (21)$$

Considering (21), it can be easily concluded that $f_{\alpha N}(t)$, $f_{\beta N}(t)$ depend only on the ratio ρ. This parameter can be experimentally fixed by measuring the back-EMFs of the PMSM [27]-[28] in MTPA strategy. This characteristic results in a high immunity of the proposed FDI process to false alarms under mechanical transient states since the obtained variables are independent from the current harmonic magnitudes.

For illustration purposes, Fig. 8 shows the fault vector propagation in α_f-β_f fault reference frame under healthy condition and when an OSF or an OPF occurs in the VSI. The obtained shapes are predicted analytically using equation (20) and verified experimentally. For the 5-Φ B-PMSM under study, the torque is produced by exciting the two fictitious machines through the first and third harmonic components. Based on the proposed algorithm, there is no path for these harmonic components in α_f-β_f fault reference frame. However, for a healthy condition, the shape is a point in the origin of this plane, as shown in Fig. 8-a. In contrast to this, after the fault occurrence, the fault vector in α_f-β_f fault reference frame describes typical shapes. Their relative positions and forms characterize the fault occurrence in original frame *abcde* and can be used as input variable of the FDI process. These positions can be easily predicted from the fault vector average position in α_f-β_f frame. Hence, as there is ten power switches in the

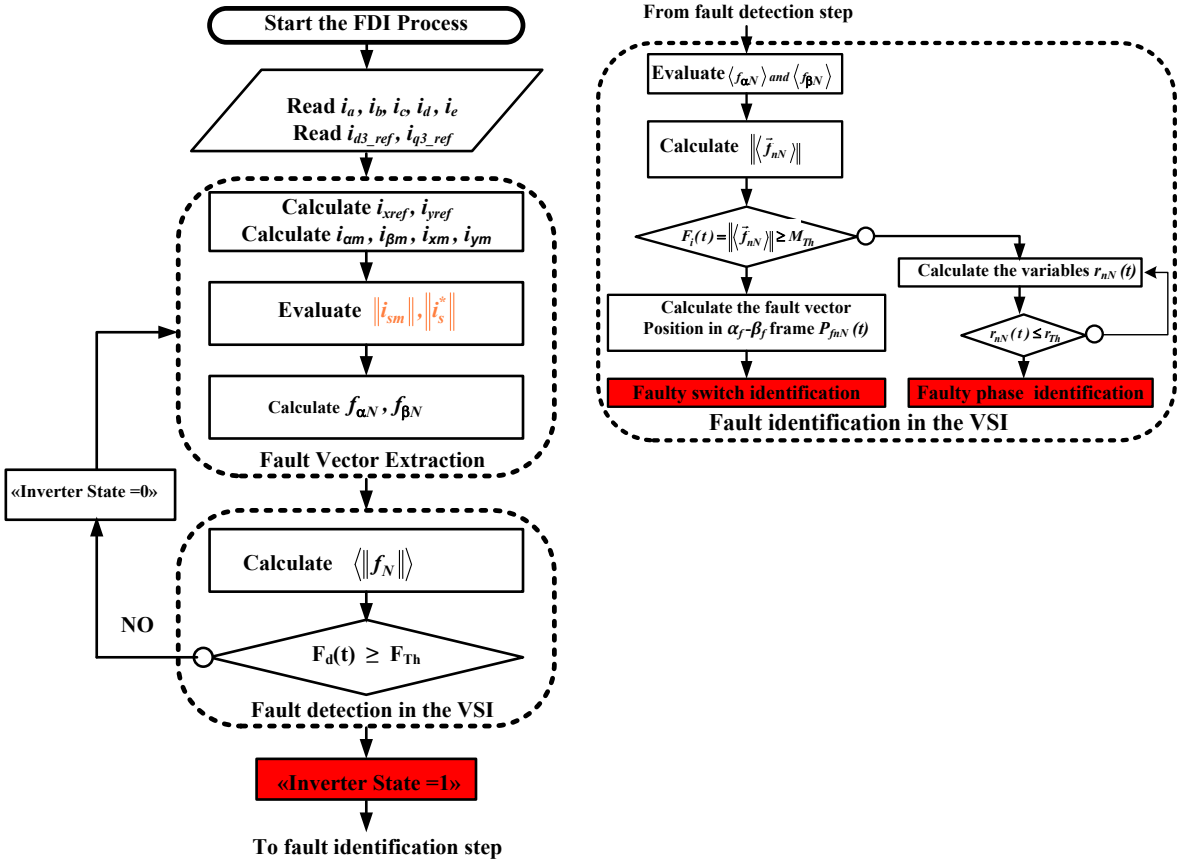

Fig. 10. Flowchart of the proposed real-time FDI process.

VSI, ten average positions of the shapes can be predicted from equation (20) according to the faulty switch location. All these positions are summarized in Fig. 9.

V. Real-Time Fault Diagnosis Algorithm

A. OSF and OPF detection and identification

In this section, the real-time FDI process is described. The flowchart of processing algorithm design is shown in Fig. 10. Firstly, five-phase currents i_a, i_b, i_c, i_d and i_e are measured. These currents together with the references derived from the control-loops are used for accurate fault vector extraction in α_f-β_f fault reference frame. To ensure the independence of the proposed FDI process of the operating conditions, an independent normalization procedure is employed for the reference and measured currents, as explained in section III. Fault detection in the VSI is achieved then by scanning α_f-β_f fault reference frame. It is defined by using the average value of the magnitude of the fault vector $\vec{f}_N$ as follows:

$$F_d(t) = \left\langle \left\| \vec{f}_N \right\| \right\rangle(t) = \frac{1}{T(t)} \int_{t-T(t)}^{T(t)} \left(f_{\alpha N}^2 + f_{\beta N}^2 \right)^{1/2} dt \tag{22}$$

A dynamic sliding window $[t-T(t); T(t)]$ is used to improve the immunity of the algorithm against false alarms and make the method as fast as possible. $T(t)$ is defined from the instantaneous real-time measured rotor speed $\Omega(t)$ as follows:

$$T(t) = \frac{2\pi}{p\Omega(t)} \tag{23}$$

Under normal operating conditions, the detection variable $F_d(t)$ is equal to zero. On the contrary, if an OSF or an OPF occurs in the VSI, the detection variable $F_d(t)$ becomes positive. The fault occurrence is judged when the magnitude of $F_d(t)$ cross a fixed threshold F_{Th} Consequently, the FDI algorithm sets the variable "inverter state" to 1, indicating thus the faulty state of the VSI.

The next step, after the fault detection, consists in identifying the first fault group, *OSG*, corresponding to the open-switch fault modes from the second fault group, *OPG*, corresponding to the open-phase fault modes in the VSI. This step is achieved by computing the magnitude of the average value of the fault vector defined as

$$F_i(t) = \left\| \left\langle \vec{f}_N \right\rangle \right\|(t) = \frac{1}{T(t)} \left\| \int_{t-T(t)}^{T(t)} \left(f_{\alpha N} + f_{\beta N} \right) dt \right\| \tag{24}$$

Considering the analysis given in section V, it is demonstrated that the first group, *OSG*, produces a half-plane shape. In this case, the variable F_i (*t*) will be positive and exceeds the threshold M_{Th}. As soon as this condition is satisfied, the FDI process calculates the fault vector average position in α_f-β_f fault reference frame over a fundamental current period, as follows:

$$P_{f_{nN}}(t) = a\tan\left(\frac{\langle f_{\beta N}\rangle(t)}{\langle f_{\alpha N}\rangle(t)}\right) = \begin{cases} (n-1)\frac{2\pi}{5}, & if \ \ f_n(t) > 0 \\ \pi + (n-1)\frac{2\pi}{5}, & if \ \ f_n(t) < 0 \end{cases} \tag{25}$$

There are ten distinct average positions of the fault vector $\vec{f}_N(t)$ according to the involved faulty switch, as addressed in Fig. 9.

On the contrary, in the case of the second group, *OPG*, the α_f- and β_f-*axis* fault vector $f_{\alpha N}$ and $f_{\beta N}$ change symmetrically over a fundamental period of current. In this situation, the direct and quadrature fault component average values are equal to zero. As a result, the variable F_i *(t)* will be zero. So, to achieve a complete diagnosis, additional variables derived also from the reference and measured currents are defined as follows:

$$r_{nN}(t) = \frac{<|\, i_{nN}\,|>(t)}{<|\, i^*_{nN}\,|>(t)} \tag{26}$$

where i_{nN} and i^*_{nN} denote the normalized quantities of the measured phase currents and the reference currents, respectively. They are given by

TABLE I
DIAGNOSTIC VARIABLES STATES FOR A HEALTHY VSI AND UNDER INVERTER OPEN-SWITCHES FAULT CONDITIONS

	Diagnostic variables with 1 < *n* < 5			
Faulty switches	**Variable $F_d(t)$**	**Variable $F_i(t)$**	**Variable $P_{f_{Nn}}(t)$**	**Variable r_{nN}**
Healthy VSI	**< F_{Th}**	**< M_{Th}**	-	1
T_n	**> F_{Th}**	**> M_{Th}**	$(n-1)2\pi/5$	
T_{n+5}	**> F_{Th}**	**> M_{Th}**	$(n-1)2\pi/5 + \pi$	-
T_n & T_{n+5}	**> F_{Th}**	**< M_{Th}**	-	0

$$i_{nN}(t) = \frac{i_n(t)}{\|i_{sm}\|}$$
$$i^*_{nN}(t) = \frac{i^*_n(t)}{\|i^*_s\|} \tag{27}$$

where $\|i_{sm}\|$ and $\left\|i_s^*\right\|$ denote, respectively, the measured current modulus and the reference current modulus. As explained in section III, the normalization procedure is achieved independently. The variables $r_{nN}(t)$ are equal to +1 under a healthy VSI. Contrariwise, they drop to zero when an open-phase occurs in the VSI and become lower than the fixed threshold r_{Th}, thus identifying the faulty phase. Table I summarizes the fault signatures which can be taken by the defined diagnostic variables when an open-switch or an open-phase occurs in the VSI.

B. Threshold Values Selection

In the proposed algorithm, there are three threshold values. These values must be carefully selected by taking into account several factors such as the transient states induced by load and speed changes, the switching noises, the sensors noises, and the levels which can be taken by the diagnostic variables for a normal operation, under an OSF or an OPF. Here, it should be noticed that all diagnostic indices are derived from normalized fault variables. Consequently, there is weak sensitivity of these indices to transient states or load and speed levels. In addition, the moving window used to compute the average values acts as a low pass filer, resulting in weak noise effect on the proposed FDI technique.

Another particular factor concerns only the multiphase bi-harmonic machines, as the 5-Φ B-PMSM under study. In this case, the torque is produced by the first and third harmonic current components. Consequently, to each operating point corresponds a fixed value of the ratio ρ defined in equation (21). This parameter must be considered for threshold values selection. The threshold values used by the algorithm are obtained by simulation and verified experimentally. Here, it is given only the experimental results of the diagnostic variables dynamic according to the variation of the ratio ρ.

Experimental results depicted in Fig. 11 show the diagnostic variables behavior according to the ratio ρ. Similar results can be predicted using the analytical model given in (20). All diagnostic variables are analyzed according to operating conditions; healthy state, OSF and OPF. Based on the obtained results, the selection of F_{Th} is achieved by analyzing the evolution of the variable F_d (t) according to the ρ ratio, as reported in Fig. 11-a. However, under a healthy state of the VSI, the variable F_d (t) is equal to zero since there is no fault component in α_f-β_f fault reference frame. On the contrary, after the fault occurrence, F_d (t) becomes positive. The exact value which can be taken by this variable varies according to parameter ρ. Hence, its minimum absolute value is equal to 0.055 regardless the speed and load levels. Based on this result, F_{Th} is fixed to universal value equal to 0.03 permitting a large dissymmetry between the healthy and the faulty modes of the VSI.

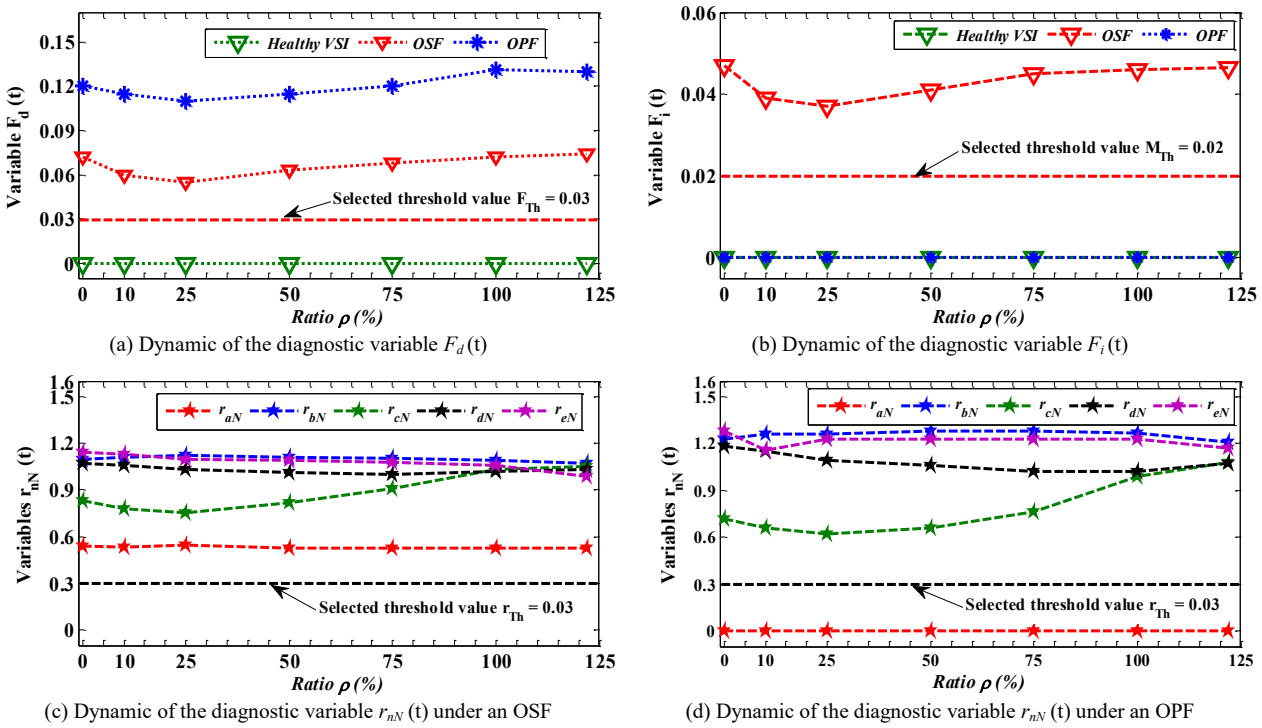

(a) Dynamic of the diagnostic variable F_d (t)

(b) Dynamic of the diagnostic variable F_i (t)

(c) Dynamic of the diagnostic variable r_{nN} (t) under an OSF

(d) Dynamic of the diagnostic variable r_{nN} (t) under an OPF

Fig. 11. Experimental results on the 5-Φ B-PMSM. Diagnostic variables behavior according to the ρ ratio under a healthy VSI and fault modes.

With similar reasoning, to select the value of the threshold M_{Th}, the dynamic of the variable F_i (t) according to the ρ ratio is considered, as reported in Fig. 11-b. From these results, it is observed that the minimum absolute value of 0.037 corresponds to an open-switch fault in the VSI. On the contrary, under a healthy condition or an OPF, F_i (t) is equal to zero. Consequently, the threshold M_{Th} is fixed to a minimum absolute value equal to 0.02.

The threshold r_{Th} is selected using the experimental results given in Fig. 11 (c-d). In these figures, it is illustrated that the diagnostic variables r_{nN} (t) are equal to +1 for a normal operation of the VSI. On the contrary, they are close to 0.5 under an OSF, and are equal to zero for an OPF in the VSI. From these results, the threshold r_{Th} is fixed to an universal value of 0.03, thus permitting a large dissymmetry between the healthy conditions and the faulty modes.

For selecting the threshold values, the impact of the current-controllers bandwidth B_{pi} and the phase impedance variations has been considered, too. For the motor under study, the typical value of the bandwidth B_{pi} is 172 Hz. Two tests are performed for B_{pi} equal to 86 Hz and 344 Hz. Based on the obtained results, it is concluded that there is no impact of this parameter on the state of the diagnostic variables. Regarding the asymmetrical phase impedance variations, it is observed that the diagnostic variables undergo a light deformation but remains always near zero. Taking into account the fixed threshold values, there is no false alarms generating by the FDI process.

VI. Experimental Results and Comments

The experimental tests are performed by using a 5-Φ B-PMSM coupled to an industrial motion drive which is used as an emulator to generate different load profiles. Fig. 12 illustrates the experimental test bench. Table II provides the parameters of the 5-Φ B-PMSM which have been used for synthesis of vector control. The proposed FDI process and the vector control algorithm are implemented in a dSPACE DS 1006 controller board with an execution step time of 40 μs. The PWM-VSI has a switching frequency of 15-kHz.

Experimental tests investigate motor behaviors and FDI Process robustness for a healthy state and during OSF and OPF occurring in the VSI. The discussion of the obtained results is addressed in the next sections.

A. FDI robustness and immunity to load and speed change

The experimental results, reported in Fig. 13, show the fault vector components in α_f-β_f fault reference frame under a healthy VSI. In this test, a change of the motor speed or the load torque is applied to the 5-Φ B-PMSM. Fig.14 provides the time-domain waveforms of the motor speed, the phase currents and the variables used for fault diagnosis in the VSI. In this evaluation, a fast transient process is conducted by a step of speed from 10 rd.s^{-1} to 50 rd.s^{-1}. The load torque is set equal to 10 N.m. Regarding the α_f-β_f plane (Fig. 13), it is observed that the trajectory built by the fault vector components in this frame is always closed to zero. The observed low magnitudes are only due to the switching and measurement noises and cannot have an impact on the robustness of the FDI process. Fig.14 demonstrates that the diagnostic variables are always within the bands that correspond to a healthy operation mode of the VSI and no false alarms are issued by this transient. These results confirm the high performance and robustness of the proposed FDI under speed change.

Fig. 15 provides the experimental results when the 5-Φ B-PMSM operates at a mechanical rotor speed equal to 50 rad/s. The transient states consist in applying to the PMSM two-step transitions of the load torque from 2 N.m to 20 N.m, and then from 20 N.m to 2 N.m. Regarding the α_f-β_f fault reference frame, it is observed that the shape built by the fault vector cannot be changed by this variation of torque. In addition, as mentioned in the above sections, in α_f-β_f fault reference frame, there is no path of the first and third current harmonic components. This characteristic is justified when considering Fig. 13 since the fault vector is always equal to zero under a healthy operation mode. As for the diagnostic variables, even though transient states are observed, they are always within the bands that correspond to a healthy operation mode of the VSI. Once more, the obtained results confirm the high performance and robustness of the proposed FDI under load change.

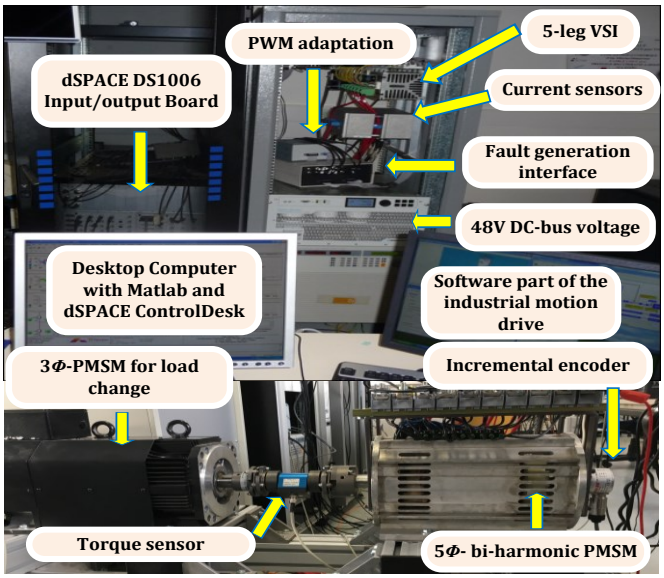

Fig. 12. Experimental test bench

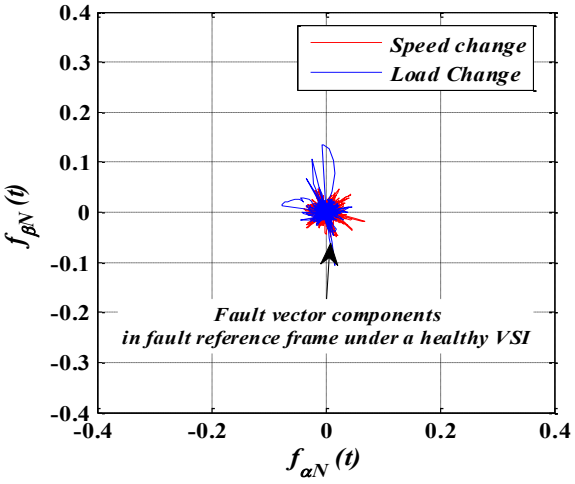

Fig. 13. Experimental result of the fault vector components in α_f-β_f fault reference frame under healthy conditions and a change of the load torque or motor speed.

TABLE II
ELECTRICAL PARAMETERS OF 5-**Φ B-PMSM**

Rs = 0.0324 Ω; *Lp* =139 *μH*; *Ls* = 178 *μH*, *p*=8, *From spectrum analysis at no load for 500 rpm, amplitudes (RMS) of emf* E_1=10,2V, E_3=13V

As in [29], the proposed algorithm in this work is based on current signature analysis (CSA). Consequently, when closed-loop control systems are used, the current-controllers bandwidth can attenuate the effect of certain faults and the disturbance on the diagnostic variables. This problem is especially observed when the diagnostic indicators are derived from the frequency components analysis, as in [29]. Fortunately, the proposed FDI process in this work is based principally on time-domain analysis of normalized fault signals, resulting in a weak modification of the shape built by the fault vector in α_f-β_f fault reference frame. As mentioned in section. V-B, the proposed algorithm is evaluated for several values of the current-controllers bandwidth *Bpi* and the obtained results confirm its independence from the variation of B_{pi}. Similar results are obtained in the case of unbalanced supply or impedance phase variation.

B. Faulty operation of the VSI and FDI effectiveness

To further examine the practicality of the proposed method, several tests are performed under fault conditions. The first test is conducted when the fault occurs in *phase a*, resulting from an open-switch fault of MOSFET T1. In this test the motor speed and the load torque are fixed, respectively, at $\Omega = 50$ rd/s and $T_{em} = 20$ N.m. Here it should be noted that the ratio ρ is fixed at 10%. However, only 12.2% of the torque is produced by a third harmonic component.

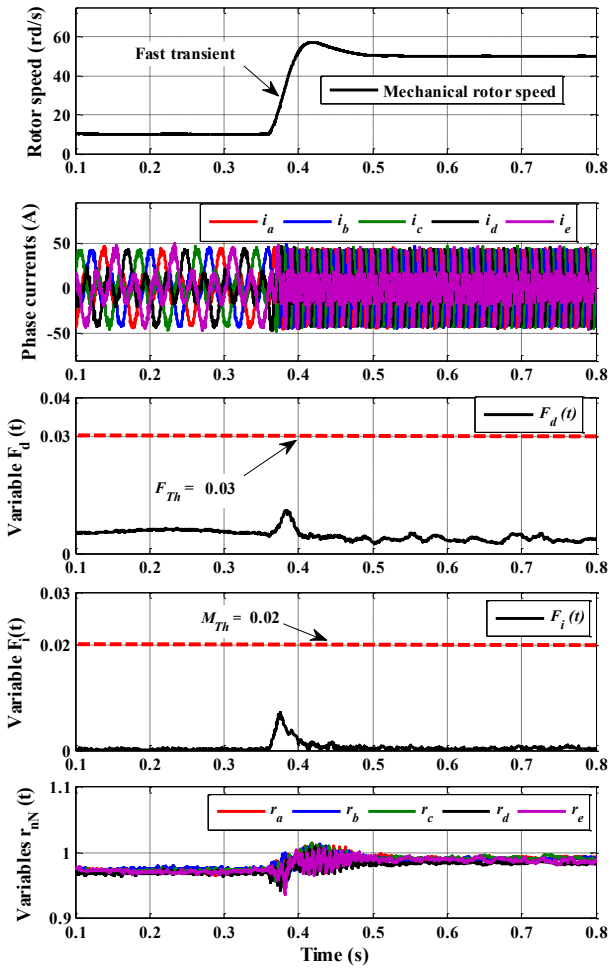

Fig. 14. Experimental results of the FDI process robustness. Time-domain waveforms of the rotor speed, the phase currents and the diagnostic variables during motor-speed change from $\Omega = 10$ rd/s to $\Omega = 50$ rd/s. T_{em}= 20 N.m. ρ=122%. (I_{h3}=1.22×I_{h1}).

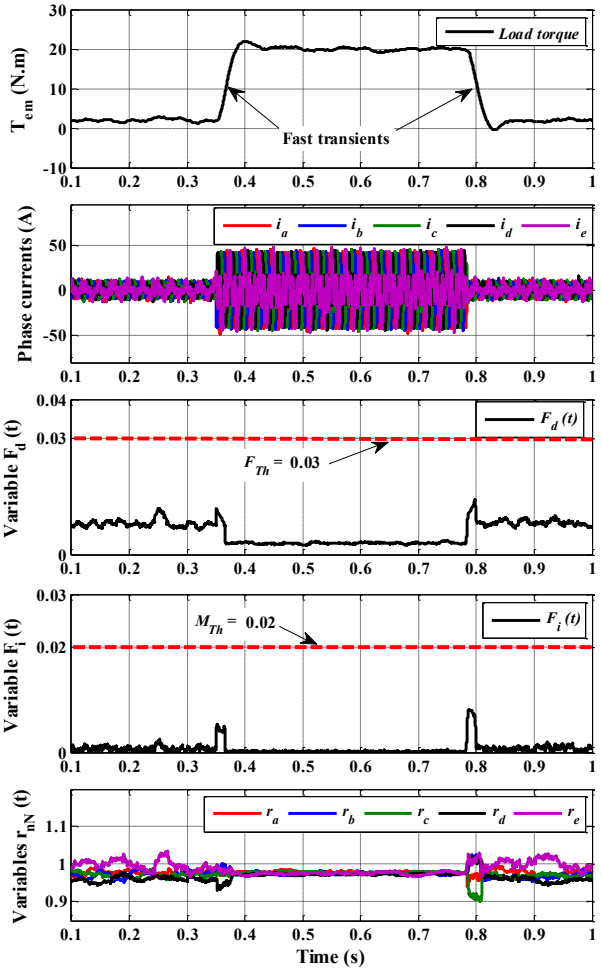

Fig. 15. Experimental results of the FDI process robustness. Time-domain waveforms of the rotor speed, the phase currents and the diagnostic variables during load torque change from Tem = 2 N.m to Tem = 20 N.m. $\Omega = 50$ rd/s. ρ=122%. (I_{h3}=1.22×I_{h1}).

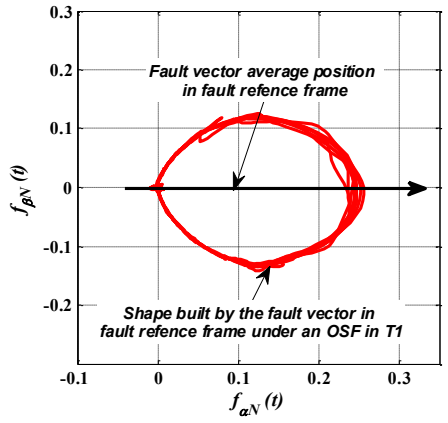

(a)

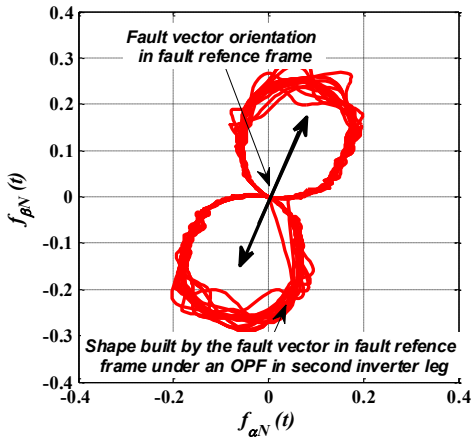

(b)

Fig. 16. Experimental result. Fault vector trajectory in α_f-β_f fault reference frame. (a) Open switch fault in T1. (b) Phase *b* open-circuit fault (T2&T7).

Firstly, the 5-Φ B-PMSM operates free of any fault which results in no fault components in α_f-β_f fault reference frame. As for the diagnostic variables, they vary within the band that corresponds to the healthy state of the VSI. At t = 0.323 s, an open-circuit fault is introduced into the transistor T1 of the first inverter leg, by permanently keeping its switching signal in "OFF" state. As a result, current i_a immediately reaches zero and is now limited to only flow in the negative direction, while other currents (*ib*, *ic*, *id*, *ie*) undergo a light deformation and flow in negative and positive directions. In α_f-β_f fault reference frame, a particular shape is built by the fault vector, as reported in Fig. 16-a. As analyzed in the theoretical part of this work, this shape effectively characterizes the fault occurrence in T1. As for the variable $F_d(t)$, it is observed that it increases immediately and exceeds the threshold F_{Th} = 0.03 corresponding to the faulty operation mode of the VSI. As a consequence, a fast fault detection is achieved at t = 0.3245 s, taking a time delay equal to almost 10% of the fundamental current period. The variable $F_i(t)$ is immediately observed to exceed the threshold M_{Th} = 0.02. As both $F_d(t)$ and $F_i(t)$ exceed their relative thresholds, the proposed algorithm makes the decision that the fault mode is an open-switch fault. However, the next step, in the diagnosis algorithm, is also achieved by using the information derived from the fault vector average position in α_f-β_f fault reference frame. It uses the variable P_{fnN} which remains around zero in the band [±10°], thus indicating that the fault is in MOSFET T1 at t = 0.325 s. As for the variables $r_{nN}(t)$, even though a light deformation is observed, they are within the level that does not correspond to any open-phase fault in the VSI ($r_{nN}(t)$>0.3). The state of these variables together with $F_d(t)$ and $F_i(t)$ successfully indicates that the fault has occurred in transistor T1.

Considering now an open-phase fault involving two transistors in the same inverter leg (T2 and T7). Fig. 18 presents the experimental results of the output-inverter currents together with the variables used for fault detection and identification in the VSI. However, the motor speed and the load torque are respectively fixed at $\Omega = 25\ \mathrm{rd/s}$ and T_{em} = 10 N.m. The ratio ρ is fixed at 122%. The fault is introduced into the second *inverter leg b* at t= 0577 s, by keeping the switching signals of both transistors T2 and T7 simultaneously in "OFF" state. In this case, current i_b becomes equal to zero over the whole current cycle. Consequently, in α_f-β_f fault reference frame, the fault vector describes a symmetrical shape corresponding to the open-circuit fault of phase *b* (Fig. 16-b). As soon as the fault occurs, the variable $F_d(t)$ exceeds the threshold F_{Th}, thus permitting a fast detection of the faulty state of the VSI at t = 0.58 s. As the shape built by the fault vector in α_f-β_f frame is symmetric, the variable $F_i(t)$ undergoes a light deformation and remains near zero without exceeding the threshold M_{Th} = 0.02. By using the fact that the normalized variable $r_{bN}(t)$ crosses a threshold r_{Th} = 0.3 and now equals zero, the diagnostic algorithm makes a decision that the

fault is an open-phase involving the second *inverter leg b*. As a result, the open-phase fault identification is achieved at t = 0.597 s.

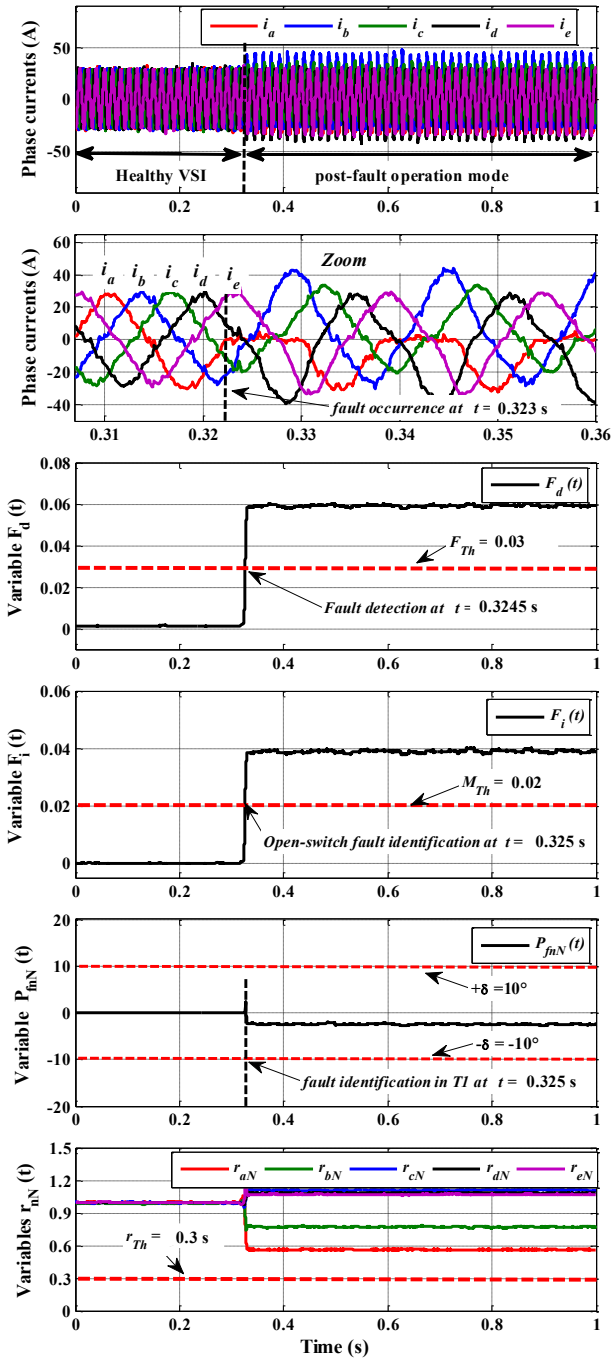

Fig. 17. Experimental results of the FDI process effectiveness. Time-domain waveforms of the phase currents and the diagnostic variables under an open-circuit fault of MOSFET T1. $\Omega = 50$ rd/s, T_{em}= 20 N. m. ρ=10% (I_{h3}=0.1×I_{h1}).

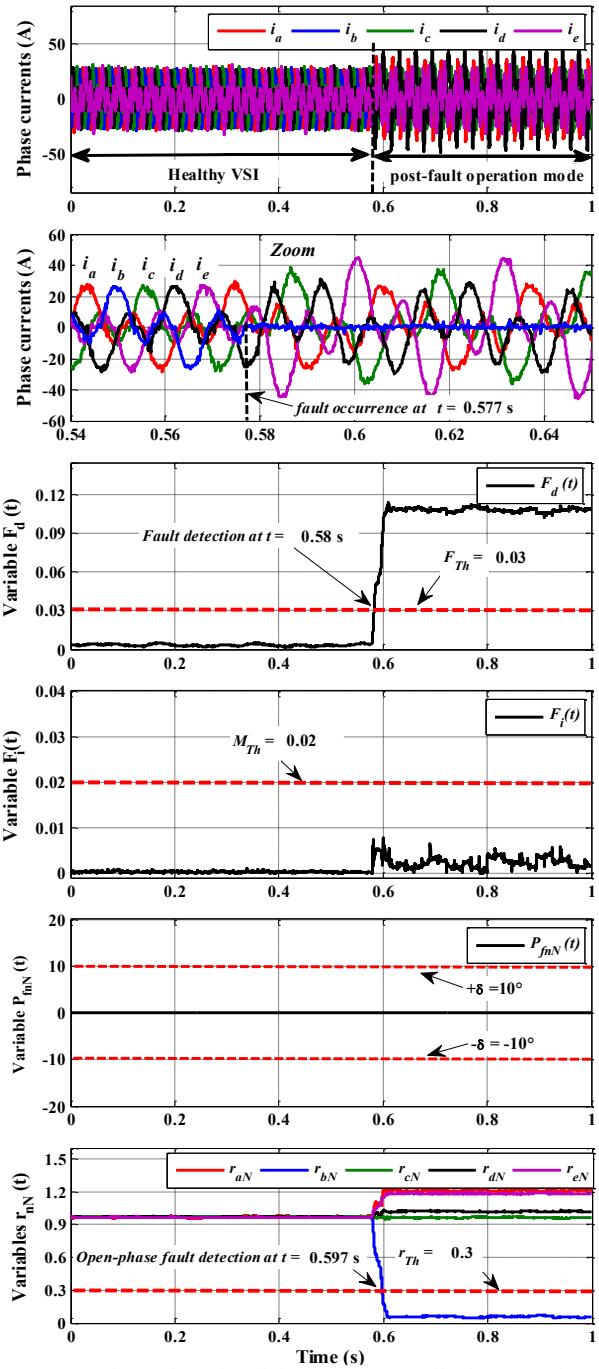

Fig. 18. Experimental results of the FDI process effectiveness. Time-domain waveforms of the phase currents and the diagnostic variables under an open-circuit fault of the motor *phase b*. $\Omega = 25$ rd/s, T_{em}= 10 N. m. ρ=122%. (I_{h3}=1.22×I_{h1}).

VII. CONCLUSION

In this paper a signal-based FDI process is proposed for inverter OSF and OPF real-time diagnosis in 5-Φ B-PMSM. Only the available current sensors are used and no-additional extra hardware is required. The proposed FDI process is based on the characteristics offered by the phase currents representation in α-β and x-y frames. By using an innovative algorithm, a 2D fault vector is defined and it is projected in a α_f-β_f fault reference frame dedicated only for fault diagnosis. In such a frame, the 2D fault vector is equal to zero under a healthy condition. On the contrary, for a faulty mode, it describes a non-zero trajectory characterizing only the open-switches faults in the VSI. The diagnostic signals are formulated on the basis of the defined frame and other variables derived from the reference and measured currents. To ensure the high immunity of the FDI process against transient states, an independent normalization procedure is employed for the reference and measured currents.

Experimental results prove the high performance of the proposed method for all operating conditions. In addition, fast fault detection and identification is achieved over almost 10% of the fundamental current cycle. The proposed FDI process can be applied to the sinusoidal and bi-harmonic 5-Φ PMSM like the system under study.

References

[1] V. I. Patel, Jiabin Wang, Weiya Wang, Xiao Chen, "Six-phase fractional-slot-per-pole-per-phase permanent-magnet machines with low space harmonics for electric vehicle application," *IEEE Trans. Indus. Electron.*, vol. 50, no. 4, pp. 2554-2563, July./Aug. 2014.

[2] X. Huang, A. Goodman, C. Gerada, F. Youtong, L. Qinfen, "Design of a five-phase brushless DC motor for a safety critical aerospace application," *IEEE Trans. Indus. Electron.*, vol. 59, no. 9, pp. 3532-3541, Sept. 2012.

[3] F. Mekri, S. Ben Elghali, M.E.H. Benbouzid, "Fault-tolerant control performance comparison of three- and five-phase PMSG for marine current turbine applications," *IEEE Trans. Sustain. Energy*, vol. 4, no. 2, pp. 425-433, April 2013.

[4] S. Yang, A. Bryant, P. Mawby, D. Xiang, L. Ran, and P. Tavner, "An industry-based survey of reliability in power electronic converters," *IEEE Trans. Ind. Appl.*, vol. 47, no. 3, pp. 1441–1451, May/Jun. 2011.

[5] R. A. Hanna, S. Prabhu, "Medium-voltage adjustable-speed drives users' and manufactures' experiences," *IEEE Trans. Indus. Appl*., vol. 33, no. 6, pp. 1407–1415, Dec. 1997.

[6] L. Bin, S. K. Sharma, "A literature review of IGBT fault diagnostic and protection methods for power inverters," *IEEE Trans Indus. Appl.*, vol. 45, no. 5, pp. 1770–1777, Oct. 2009.

[7] B. Mirafzal, "Survey of fault-tolerance techniques for three-phase voltage source inverters," *IEEE Trans. Indus. Electron*., vol. 61, no. 10, pp. 5192-5202, Oct. 2014.

[8] N. K. Nguyen, F. Meinguet, E. Semail, X. Kestelyn, "Fault-tolerant operation of an open-end winding five-phase PMSM drive with short-circuit inverter fault," *IEEE Trans. Indus. Electron*., vol. 63, no. 1, pp. 595-605, Jan. 2016.

[9] Z. Gao, C. Cecati, S. X. Ding, "A survey of fault diagnosis and fault-tolerant techniques—Part 1: fault diagnosis with model-based and signal-based approaches," *IEEE Trans. Indus. Electron*., vol. 62, no. 6, pp. 3757-3767, Jun. 2015.

[10] Q-T An, L-Z Sun, K. Zhao, L. Sun, "Switching function model based fast diagnostic method of open-switch faults in inverters without sensors," *IEEE Trans. Power Electron.*, vol. 26, no. 1, pp. 119-126, Jan. 2011.

[11] M. Trabelsi, M. Boussak, M. Gossa, "PWM-switching pattern-based diagnosis scheme for single and multiple open-switch damages in VSI-fed induction motor drives," *ISA Trans.*, vol. 51, pp. 333-344, 2012.

[12] F. Wu, J. Zhao, "A real-time multiple open-circuit fault diagnosis method in voltage-source-inverter fed vector controlled drives," *IEEE Trans. Power Electron.*, vol. 31, no. 2, pp. 1425-1437, Feb. 2016.

[13] W. Sleszynski, J. Nieznanski, A. Cichowski, "Open-transistor fault diagnostics in voltage-source inverters by analyzing the load currents," *IEEE Trans. Indus. Electron.*, vol. 56, no. 11, pp. 4681-4688, Nov. 2009.83.

[14] J. O. Estima, A. J. Marques Cardoso, "A new algorithm for real-time multiple open-circuit fault diagnosis in voltage-fed PWM motor drives by the reference currents errors," *IEEE Trans. Indus. Electron.,* vol. 28, no. 5, pp. 3496-3505, Aug. 2013.
[15] J. O. Estima, A. J. Marques Cardoso, "A new approach for real-time multiple open-circuit fault diagnosis in voltage-source inverters," *IEEE Trans. Indus. Appl.*, vol. 47, no. 6, pp. 2487-2494, Nov./Dec. 2011.
[16] B. G. Park, K. J. Lee, R. Y. Kim, T. S. Kim, J. S. Ryn, D. S. Hyun, "Simple fault diagnosis based on operating characteristic of brushless direct-current motor drives," *IEEE Trans. Indus. Electron*., vol. 58, no. 5, pp. 1586-1593, Feb. 2011.
[17] Q. T. An, L. Z. Sun, K. Zhao, and L. Sun, "Current residual vector-based open-switch fault diagnosis of inverters in PMSM drive systems," *IEEE Trans. Power Electron.*, vol. 30, no. 5, pp. 2814–2827, May 2015.
[18] S. M. Jung, J. S. Park, H.W. Kim, K. Y. Cho, and M. J. Youn, "An MRAS based diagnosis of open-circuit fault in PWM voltage source inverters for PM synchronous motor drive systems," *IEEE Trans. Power Electron.*, vol. 28, no. 5, pp. 2514–2526, May 2013.
[19] I. Jlassi, J. O. Estima, S. K. El Khil, N. M. Bellaaj, and A. J.Cardoso, "Multiple open-circuit faults diagnosis in back-to-back converters of PMSG drives for wind turbine systems," *IEEE Trans. Power Electron.*, vol. 30, no. 5, pp. 2689–2702, May 2015.
[20] D. U. Campos-Delgado and D. R. Espinoza-Trejo, "An observer-based diagnosis scheme for single and simultaneous open-switch faults in induction motor drives," *IEEE Trans. Ind. Electron.*, vol. 58, no. 2, pp. 671–679, Feb. 2011.
[21] M. Salehifar, R. S. Arashloo, J. M. Moreno-Equilaz, V. Sala, L. Romeral, "Fault detection and fault tolerant operation of a five phase PM motor drive using adaptive model identification approach," *IEEE J. Emerging Sel. Top. Power Electron*, vol. 2, no. 2, pp. 212-223, Jun. 2014.
[22] M. Trabelsi, N. K. Nguyen, E. Semail, "Real-time switches fault diagnosis based on typical operating characteristics of five-phase permanent magnetic synchronous machines," *IEEE Trans. Indus. Electron.*, vol. 63, no. 8, pp. 4683-4694, Aug. 2016.
[23] H. Guzman, M. J. Duran, F. Barrero, L. Zarri, B. Bogado, I. Gonzalez, Manuel R. Arahal, "Comparative study of predictive and resonant controllers in fault-tolerant five-phase induction motor drives," *IEEE Trans. Indus. Electron.*, vol. 63, no. 1, pp. 606-617, Jan. 2016.
[24] M. Trabelsi, E. Semail, N. K. Nguyen, F. Meinguet, "Open-switch fault effects analysis in five-phase PMSM designed for aerospace application", *In Proc. of IEEE-SPEEDAM'2016,* Italy, Jun.2016.
[25] F. Scuiller, H. Zahr, E. Semail, "Maximum reachable torque, power and speed for five-phase SPM machine with low armature reaction," *IEEE Trans.Energy Convers.,* vol.31, no.3, pp.959-969, 2016.
[26] H. Zahr, J. Gong, E. Semail, F. Scuiller, "Comparison of optimized control strategies of a high-speed traction machine with five phases and bi-harmonic electromotive force," *Energies*, vol.9, no. 12, pp. 1-9, 2016.
[27] X. Kestelyn, E. Semail , "Vectorial modeling and control of multiphase machines with non-salient poles supplied by an inverter", Chap.5 in book " Control of non-conventional synchronous motors", ISTE Ltd and John Wiley & Sons Inc, 2012, 44 pages.
[28] X. Kestelyn, E. Semail, "A vectorial approach for generation of optimal current references for multiphase permanent-magnet synchronous machines in real time," *IEEE Trans. Ind. Electron.*, vol. 58, no. 11, pp. 5057-5065, Nov. 2011.
[29] Y. Gritli, A. Tani, C. Rossi, D. Casadei, "Closed-loop control impact on condition monitoring of high-resistance connections in PMSM based on power signature analysis," in *Proc. 42th IECON*, Oct. 2016, pp. 6966-6970.

Mohamed Trabelsi (M'16) received the B.S. and M.S. degrees in electrical engineering from the Ecole Superieure des Sciences et Techniques, University of Tunis, Tunis, Tunisia, in 2005 and 2007, respectively, and the Ph.D. degree in electrical engineering jointly from the Aix-Marseille University, Marseille, France, and the Ecole Superieure des Sciences et Techniques, University of Tunis, in 2012. He is currently a Postdoctoral with Ecole Nationale Superieure des Arts et Metiers (ENSAM), Laboratory of Electrical Engineering and Power Electronics of Lille (L2EP), Arts et Metiers ParisTech, Lille, France. He is also an Associate Professor of electrical engineering with the Ecole Nationale d'Ingenieurs de Sousse, ENISO, Sousse, Tunisia. His research interests include modeling, control, and diagnostics of conventional three-phase ac motor drives, power converters, and multiphase drives.

Eric Semail (M'02) graduated from the Ecole Normale Superieure, Paris, France, in 1986, and received the Ph.D. degree with a thesis entitled "Tools and studying method of polyphase electrical systems—Generalization of the space vector theory" from the University of Lille, France, in 2000. He became an Associate Professor at the Engineering School of Arts et Metiers

ParisTech, Lille, France, in 2001 and a Full Professor in 2010. In the Laboratory of Electrical Engineering of Lille (L2EP), France, his fields of interest include design, modeling, and control of multiphase electrical drives (converters and ac drives). More generally, he studies, as a Member of the Control team of L2EP, multimachine and multiconverter systems. Fault tolerance for electromechanical conversion at variable speeds is one of the applications of the research with industrial partners in fields such as automotive, marine, and aerospace. Since 2000, he has collaborated on the publication of 27 scientific journals, 64 International Congresses, 5 patents, and 2 chapters in books.

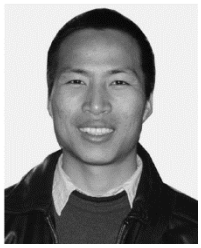

Ngac Ky Nguyen (M'13) received the B.Sc. degree in Electrical Engineering from Ho Chi Minh City University of Technology, Vietnam, in 2005, and the Ph.D. degree in Electrical and Electronic engineering from the University of Haute Alsace, France, in 2010. Since September 2012, he has been an Associate Professor with the Laboratory of Electrical Engineering and Power Electronics of Lille, Arts et Métiers ParisTech, Lille, France. His research interests include Modeling and Control of Synchronous Motors, Power Converters, and Fault-Tolerant Multiphase Drives. He has authored and co-authored 38 scientific papers and 5 book chapters.